The Journal of Experimental Biology 211, 1603-1611
Published by The Company of Biologists 2008
doi:10.1242/jeb.013250

Thunniform swimming: muscle dynamics and mechanical power production of aerobic fibres in yellowfin tuna (*Thunnus albacares*)

Robert E. Shadwick[1,*] and Douglas A. Syme[2]

[1]Department of Zoology, University of British Columbia, Vancouver, BC, V6T 2A9, Canada and [2]Department of Biological Sciences, University of Calgary, Calgary, AB, T2N 1N4, Canada

*Author for correspondence (e-mail: shadwick@zoology.ubc.ca)

Accepted 20 March 2008

SUMMARY

We studied the mechanical properties of deep red aerobic muscle of yellowfin tuna (*Thunnus albacares*), using both *in vivo* and *in vitro* methods. In fish swimming in a water tunnel at 1–3 *L* s^{-1} (where *L* is fork length), muscle length changes were recorded by sonomicrometry, and activation timing was quantified by electromyography. In some fish a tendon buckle was also implanted on the caudal tendon to measure instantaneous muscle forces transmitted to the tail. Between measurement sites at 0.45 to 0.65 *L*, the wave of muscle shortening progressed along the body at a relatively high velocity of 1.7 *L* per tail beat period, and a significant phase shift (31±4°) occurred between muscle shortening and local midline curvature, both suggesting red muscle power is directed posteriorly, rather than causing local body bending, which is a hallmark of thunniform swimming. Muscle activation at 0.53 *L* was initiated at about 50° of the tail beat period and ceased at about 160°, where 90° is peak muscle length and 180° is minimum length. Strain amplitude in the deep red fibres at 0.5 *L* was ±5.4%, double that predicted from midline curvature analysis. Work and power production were measured in isolated bundles of red fibres from 0.5 *L* by the work loop technique. Power was maximal at 3–4 Hz and fell to less than 50% of maximum after 6 Hz. Based on the timing of activation, muscle strain, tail beat frequencies and forces in the caudal tendon while swimming, we conclude that yellowfin tuna, like skipjack, use their red muscles under conditions that produce near-maximal power output while swimming. Interestingly, the red muscles of yellowfin tuna are slower than those of skipjack, which corresponds with the slower tail beat frequencies and cruising speeds in yellowfin.

Key words: muscle strain, muscle power, red muscle, work loop, swimming, yellowfin tuna.

INTRODUCTION

Tunas are interesting examples of an extreme design for aquatic locomotion, and are highly convergent with lamnid sharks in terms of their specialized anatomy and physiology, and their roles as apex pelagic predators (reviewed by Bernal et al., 2001; Donley et al., 2004; Shadwick, 2005). These features include a highly streamlined body, elevated core temperatures, concentration of aerobic red muscle to anterior and medial positions, and high sustained swimming speeds powered primarily by lateral motion of the hydrofoil-like tail rather than body undulations (Bernal et al., 2001; Graham and Dickson, 2000; Graham and Dickson, 2004). Despite their innate appeal to comparative physiologists, studies on muscle function in tunas during swimming are sparse, undoubtedly because laboratory access for research on live specimens is very limited. In work carried out at the Kewalo Research Facility in Hawaii we discovered an anomalous relation between actual muscle shortening and that predicted based on midline curvature in skipjack tuna (*Katsuwonis pelamis*), which appears to underpin the thunniform mode of swimming (Shadwick et al., 1999). We also found that red muscle shortening in yellowfin tuna (*Thunnus albacares*) is greater than expected based on the degree of body bending (Katz et al., 2001), suggesting that the location of red muscle close to the backbone does not limit shortening nor impose a mechanical disadvantage as previously anticipated (Shadwick, 2005). Indeed, by having red muscle positioned close to the backbone and away from direct linkage to the skin these fibres can produce greater, rather than less, contractile work and power for swimming because of greater shortening and long-reaching tendon linkages.

There is further evidence that thunniform swimmers use their red muscles for propulsion under near-optimal conditions for power production. The impact of regional endothermy on muscle performance in yellowfin tuna was investigated using cyclic contractions on isolated segments of red muscle (work loop technique) with optimized activation parameters (Altringham and Block, 1997). Their study showed that power output was highly temperature dependent, and that an elevation of core temperature by 10°C would typically double the maximum muscle power output and the frequency at which it occurs, providing a basis for fast, sustained swimming due to their ability to retain muscle heat. Additional evidence for muscle power enhancement in yellowfin tuna was presented in a preliminary report of a work loop study using strain and activation timing derived from measurements in swimming fish (Katz et al., 2001). Subsequently, we investigated muscle contractile properties in skipjack tuna (*K. pelamis*) by the work loop technique and concluded that red muscle fibres along the entire body are used in a similar fashion to produce near-maximal mechanical power for propulsion during normal cruise swimming (Syme and Shadwick, 2002).

In the present study we examine muscle dynamics in yellowfin tuna by the use of sonomicrometry and electromyography in swimming fish, and by the work loop technique on isolated bundles of muscle fibres *in vitro*. We present an analysis of the performance

of aerobic muscle in swimming, and draw comparisons to previous data for skipjack tuna. We note that both species display a phase shift between red muscle strain and midline curvature, a hallmark of thunniform swimming, that both yellowfin and skipjack tuna appear to use their red muscles in a manner that is nearly optimal for power output while swimming, and that the red muscles of yellowfin tuna are slower than those of skipjack, corresponding to the slower tail beat frequencies in yellowfin and the larger pectoral fins that provide lift.

MATERIALS AND METHODS

Experiments were conducted at the National Marine Fisheries Service, Kewalo Research Facility in Honolulu, Hawaii, USA. Yellowfin tuna *Thunnus albacares* Bonnaterre 1788, 0.39–0.54 m fork length (*L*), were caught on barbless hooks by commercial fishermen and transferred to 30 000 l holding tanks with minimal physical handling. The tanks had a continuous supply of fresh seawater (24–26°C) and aeration. Tuna were fed daily with chopped squid and fish until satiated. *In vivo* experiments were conducted on healthy, feeding fish that had been held for a minimum of 1 week after capture. Some *in vitro* experiments were conducted on fish within the first week of captivity. All care and experimental procedures were carried out according to University of California approved protocols.

In vivo muscle dynamics

Sonomicrometry was used to measure muscle length changes in the deep red muscle of yellowfin tuna while they swam in a calibrated water tunnel treadmill. The details of the techniques are described elsewhere (Shadwick et al., 1999). In brief, fish were anesthetized quickly by submergence in well-oxygenated seawater containing 1 g l^{-1} tricaine methanesulphonate (Argent Chemical, Redmond, WA, USA) buffered to pH 7.8 with Tris base (Sigma) for 2–3 min, then transferred to a lower maintenance dose of 0.057 g l^{-1} and ventilated while surgery was performed. Piezoelectric sonomicrometry crystal pairs were implanted in deep red muscle at axial locations between 0.45 *L* and 0.65 *L via* an entry point near the dorsal midline (see Fig. 1). This approach was necessary to avoid damage to the vascular rete, which is situated lateral to the red muscle loin. Each pair was separated by 8–15 mm along the body axis and correct crystal alignment was ensured by monitoring the RF signal with an oscilloscope. In six fish, 34-gauge insulated copper wire electrodes with 1 mm bare tips were also implanted in the red muscle next to the crystals to monitor muscle activity. Placement of electrodes and location of the crystals were determined by post-mortem examination. In four fish muscle force was measured with a buckle force transducer fixed on the caudal tendons (see Fig. 1). Details of this procedure, including calibration, are given elsewhere (Knower et al., 1999). After surgery the fish were revived by ventilation with clean seawater in the water tunnel, and swimming trials were conducted over the range of speeds at which the fish were willing to swim (0.7–3.5 *L* s^{-1}). Sonometric signals were processed by a Triton system-6 sonomicrometry unit. EMG signals were conditioned with a Grass P15 amplifier using a bandwidth of 30–300 Hz. Both signals were recorded digitally on a microcomputer at 1000 Hz using a TL-2 interface and Axotape software (Axon Instruments, Foster City, CA, USA). Simultaneous video images of the dorsal silhouette of the swimming fish against a reflective background were collected at 60 Hz and 0.001 s shutter speed with a CCD camera. The excitation voltage of a flashing red diode visible in the video image was recorded and used for data synchronization.

Data analysis

The relation between swimming speed and tail beat frequency (*f*) was quantified. Average frequency at each speed was calculated from the time for 10–20 consecutive tail beats in each bout, and speed was expressed in *L* s^{-1}. Stride length, defined as the distance travelled in one tail beat cycle, was calculated by dividing swimming speed by *f*. Based on criteria of high signal-to-noise ratio, correct crystal placement and steady swimming, we selected muscle length and EMG data from six trials of five fish for analysis of muscle activation timing. Muscle length signals were low-pass filtered and corrected for the 5 ms delay introduced by the output filter of the sonomicrometer. Strain was calculated by subtracting mean length from the length signal and then dividing by the mean length. EMG signals were filtered and processed digitally to determine onset and offset times relative to the muscle strain cycle, as described previously (Knower et al., 1999; Donley and Shadwick, 2003).

Kinematic analyses of body bending were performed for eight swimming bouts of at least eight consecutive tail beats from four fish, according to the bending beam model we used previously (Katz et al., 1999; Shadwick et al., 1999; Donley and Shadwick, 2003). This consisted of fitting polynomial curves to the dorsal midline of each video field in a bout, and then calculating curvature as a function of time at the axial position where sonomicrometry crystals were placed. Multiplication of curvature by the horizontal distance between the crystals and the backbone yielded a prediction of axial strain, based on the equation for a bending beam (van Leeuwen et al., 1990). This result was then compared in phase to the muscle strain waveform from sonomicrometry by using a Fourier transformation technique (see Katz and Shadwick, 1998).

In six fish we successfully recorded muscle strain at two or three axial locations simultaneously. In these cases, the phase shift (and hence Δt) between adjacent strain waveforms was determined by Fourier transformation of 10–20 successive tail beats per swimming bout, and then the axial speed of the strain wave on the body was computed.

In vitro muscle contractile properties

Muscle fibre bundles were prepared for use in work-loop experiments as in previous studies (Katz et al., 2001; Syme and Shadwick, 2002). Fish were captured with a dip net and immediately killed with a blow to the head followed by severing of the spinal cord. A slab of muscle was cut from the side of the fish, extending laterally through the deep loin of red muscle, and from this blocks of 2–5 myomeres were dissected at 0.5 *L* (*N*=5) and 0.65 *L* (*N*=3). In two cases bundles of white muscle were also successfully prepared. Samples were pared to a single myomere with a fibre bundle approximately 0.5 mm in diameter and strips of myosepta at each end. Dissections were done at 5–10°C. The muscle was rinsed frequently with chilled saline during dissections (composition, in mmol l^{-1}: NaCl, 175.5; KCl, 2.6; $CaCl_2$, 2.7; $MgCl_2$, 1.1; sodium pyruvate, 10; Hepes, 10; pH 7.8 at 25°C, saturated with pure oxygen). Fibre bundles were transferred to an acrylic chamber filled with circulating saline at 25°C and bubbled with oxygen. The myoseptum at one end was tied to a stainless steel pin on a servomotor arm (Cambridge Technology, model 350, Lexington, MA, USA) and the other end was tied to a pin extending from a force transducer (AE801, SensoNor, Horten, Norway). The sample was stretched to remove visible slack. A platinum-tipped stimulating electrode was used to provide a stimulus, and voltage was increased until a maximal isometric twitch was elicited (4 ms pulse duration), and this was then increased by 50% to ensure maximal activation of the preparation. The *in vivo* muscle mean length l_0 was

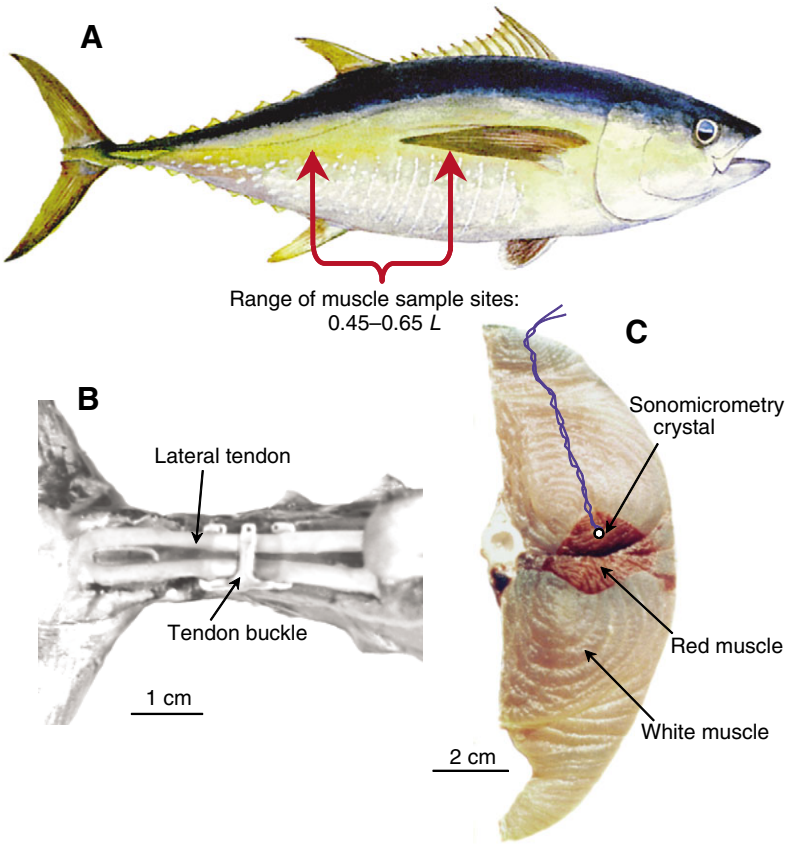

Fig. 1. (A) Lateral view of a yellowfin tuna, indicating the region where sonomicrometry and muscle fibre sample sites were located (0.45–0.65 *L*, where *L* is fork length). (B) View of caudal penduncle with skin removed showing lateral tendons that transmit forces from the muscle to the tail and the tendon buckle transducer used to measure force in the tendons. (C) View of one side of a yellowfin in cross-section at 0.55 *L* showing the deep location of the aerobic red muscle and illustrating the positioning of a sonomicrometer crystal in the red muscle.

approximated by a combination of isometric force and work recordings; sample length was adjusted so that developed twitch force and work were near maximal and passive tension during work recordings was not excessive. A stimulus frequency of 40 Hz gave maximal, isometric, tetanic force and was used during all subsequent measurements of force and work.

Work and power recordings

Mechanical work and power were determined using the work-loop method (Josephson, 1985) as described previously for skipjack tuna (Syme and Shadwick, 2002). The servomotor imposed a small sinusoidal length change centered about l_0. The peak-to-peak amplitude of the length change, expressed as a percent of l_0, is the strain amplitude. During each cycle the muscle was stimulated phasically so that force was developed primarily during shortening and the muscle was relaxed during lengthening. Stimulus phase is the time during the strain cycle that the stimulus began, and is expressed in degrees of a cycle, with 0° representing lengthening through l_0, 90° the maximum length and 270° the minimum length. Work and power were measured over a range of cycle frequencies that encompassed the tail beat frequencies observed in swimming yellowfin tuna of similar size. Strain amplitude used was ±5.5%, based on *in vivo* measurements (Shadwick et al., 1999) (and see below) and ±2.75%, based on midline curvature (see Table 1). A strain of ±8% was also tested at 3 Hz to further assess the effects of strain amplitude on work and power. For each frequency and strain combination, stimulus duration and phase were systematically altered until the net work produced by the muscle was maximal. Stimulus phase and duration measured *in vivo*, based on EMG recordings in swimming fish, were compared to optimal.

Samples were subjected to three cycles of strain and stimulation at each combination of parameters studied; measurements were taken from the second or third cycle, whichever was greater. Work was calculated as the integral of force with respect to muscle length over the complete sinusoidal strain cycle. Power is the rate of doing work and equals work per cycle times the cycling frequency. Isometric tetanic force was monitored regularly during the experiments, and used to adjust work values for fatigue or gradual deterioration of the preparation, assuming a linear relationship between any change in force and work between recordings (e.g. Coughlin, 2000; Altringham and Young, 1991; James et al., 1995; Altringham and Block, 1997; Ellerby et al., 2001). We found that the isometric force declined over the course of the experiments by 21.6±13.9% (mean ± s.d.) of the initial value. For comparative purposes we expressed work and power in mass-specific units, following the method used previously (Katz et al., 2001; Syme and Shadwick, 2002). Briefly, since determining the samples' mass or volume is confounded by their very small size, irregular dimensions, and uncertainties about the proportion of viable cells, we calculated active cross-sectional area based on the assumption that live fibres could generate 140 kN m^{-2} maximal, isometric, tetanic stress. This area, in conjunction with the length of the fibre bundle, was used to calculate muscle mass, assuming a muscle tissue density of 1050 kg m^{-3}. These assumptions mean that comparisons of mass-specific power with other preparations should be made with caution, but relative changes in work and power are independent of this calculation.

RESULTS

Body kinematics and muscle dynamics

The yellowfin used in this study swam continuously and undisturbed in their 7 m diameter holding tanks at an average tail beat frequency (f) of 1.97±0.24 Hz (N=6), as determined from video analysis. In forced water-tunnel swimming over a range of speeds there was a linear relation between normalized swimming speed and f (Fig. 2A). Based on this regression, the routine cruising speed in holding tanks was approximately 1 *L* s^{-1}, close to the slowest speeds that fish would tolerate in the water tunnel and slightly above the minimum needed to maintain hydrostatic equilibrium (Magnuson, 1978). Stride length increased non-linearly with speed, as expected, reaching values of 0.6–0.7 at cruising speeds of 2–3 *L* s^{-1} (Fig. 2B). These values are similar to those from other studies of swimming fish including tunas (Altringham and Shadwick, 2001; Shadwick and Gemballa, 2006).

Examples of segment length changes in the deep aerobic muscle, measured by sonomicrometry, are shown in Fig. 3A. In this case, length signals recorded at three locations illustrate that there is a short time delay associated with the progression of muscle contractions along the body (Fig. 3B). Calculation of the axial strain

wave speed yields a range of values that are positively correlated to swim speed, when expressed in units of L s^{-1} (Fig. 4).

When we compared the deep red muscle strain as measured by sonomicrometry with that calculated from body curvature we observed two notable differences, illustrated in Fig. 5 and Table 1. First, the measured strain amplitude at mid-body was about twice the predicted value (±5.4% *vs* ±2.7%; Table 1). Second, the measured strain wave was temporally delayed relative to the local body curvature by nearly 10% of a tail beat cycle (31.0±3.7°; Table 1). Based on the axial speed of the strain wave and curvature analysis at more posterior locations (data not shown) we calculated that contractions of deep red muscle at 0.5 L were coincident with bending at approximately 0.7–0.75 L (see also Katz et al., 2001).

In vivo muscle activation and force

Fig. 6 shows an example of simultaneous recordings of EMG activity and segment length changes in deep red muscle at 0.5 L. This type of data was used to determine the average phase of muscle activation onset and termination, and hence the duration or duty cycle of muscle activity in five fish (see Table 2). Fig. 7 shows an example of force recorded in lateral caudal tendons of one yellowfin swimming at 2.2 L s^{-1} in which muscle strain at 0.5 L was also recorded. Previous kinematic analysis of skipjack tuna showed that muscle strain in mid-body is in phase with lateral motion of the caudal fin, so here we plotted the force in the caudal tendons and mid-body muscle strain to obtain an *in vivo* 'work loop'. This shows large, positive net work, similar to the *in vitro* work loops recorded from red muscle of this species (see Figs 8, 9 below) as well as from skipjack tuna with activation and strain conditions that mimic those recorded *in vivo* (Syme and Shadwick, 2002).

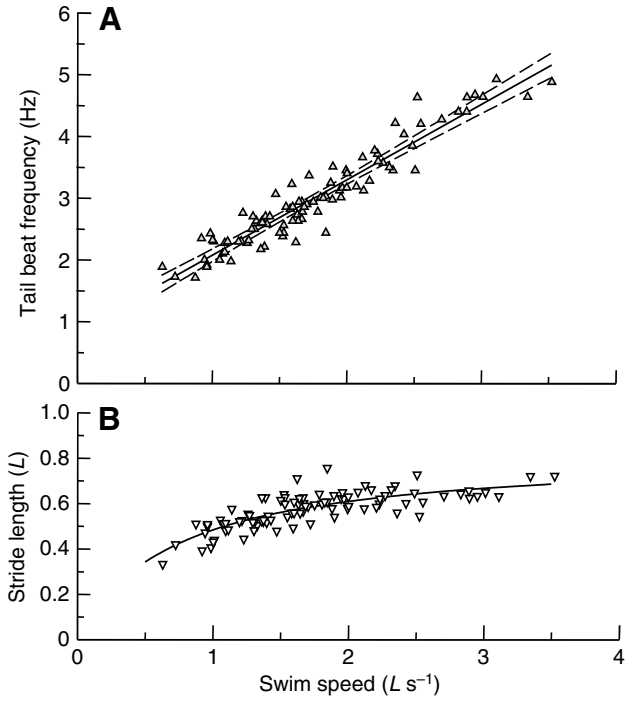

Fig. 2. (A) Summary of tail beat frequency *vs* swim speed for 95 swimming bouts from 12 yellowfin tuna used in this study (mean length=0.450±0.05 m; mean mass=1.53±0.54 kg). Solid line is a fitted regression (y=1.22x+0.85; R^2=0.91) with 95% confidence intervals (broken lines). (B) Stride length *vs* swim speed derived from data in A.

In vitro red muscle work and power

Red muscle samples taken from 0.5 and 0.65 L generated large work loops with positive net work output at cycle frequencies of 1–4 Hz at 25°C when stimulus phase and duration were optimized for maximum work (Figs 8, 9). Net work per cycle peaked at 2 Hz and

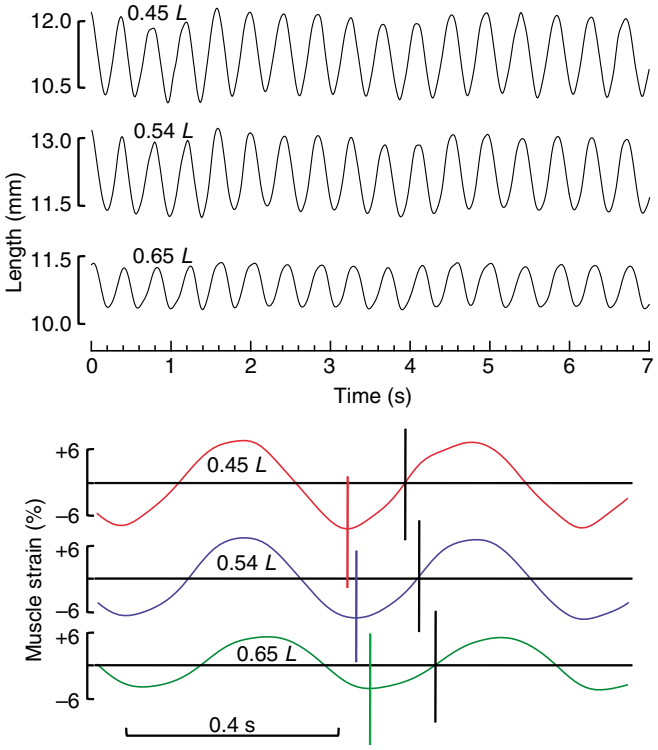

Fig. 3. (A) Example of length changes recorded by sonomicrometry in red muscle at three axial positions in a 54 cm yellowfin tuna swimming at 1.3 L s^{-1}. (B) Expanded section of traces in A with length changes expressed as % strain. Vertical lines show the progressive time delay from anterior to posterior positions: coloured lines indicate time of minimum muscle length during the cycle, black lines indicate time that the muscle passed through resting length.

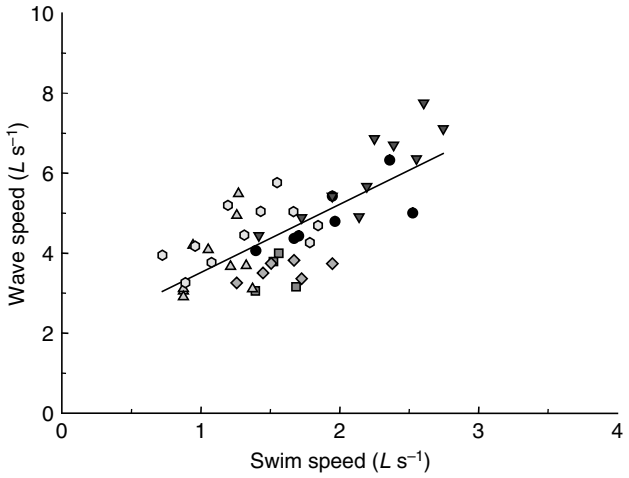

Fig. 4. Velocity of strain wave in deep red muscle, calculated as the distance between recording sites divided by the time shift (N=6; R^2=0.59). Each individual is represented by a different symbol.

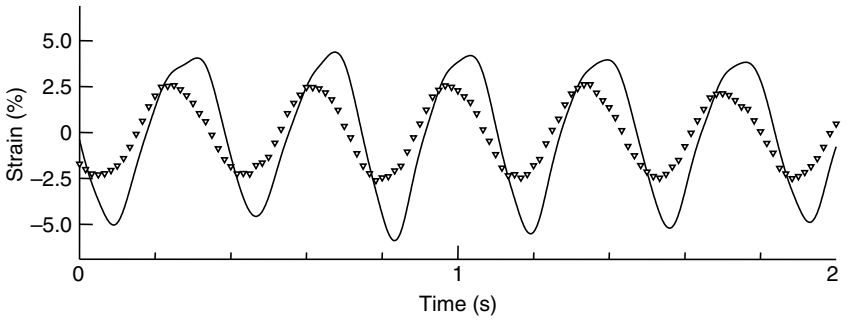

Fig. 5. Comparison of red muscle strain at 0.5 *L* measured by sonomicrometry (solid line) *vs* strain calculated from midline curvature (symbols). Note these two waveforms differ in amplitude and phase.

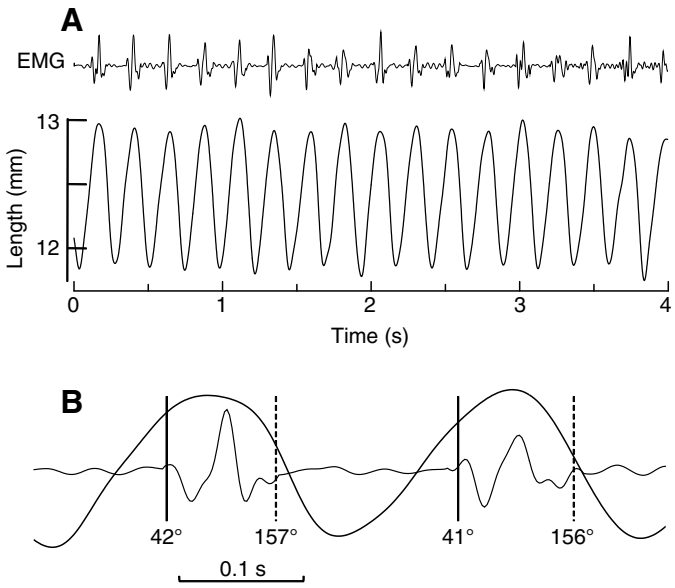

Fig. 6. Example of EMG and length change in red muscle at 0.5 *L* of a 39 cm yellowfin tuna swimming at 2.6 *L* s^{-1}. (A) Sixteen consecutive tail beat cycles during steady swimming. (B) Expanded time scale for two typical cycles showing that muscle activation begins during the latter part of lengthening (solid vertical lines) and ends about half way through shortening (broken vertical lines). Activation phases for these two cycles are indicated.

Table 1. Muscle strain amplitude (as ±% of mean length) for tuna deep red muscle at mid-body (0.5±0.01 *L*) measured by sonomicrometry and calculated from midline curvature

Strain amplitude, measured by sonomicrometry	5.4±1.58%
Strain amplitude, predicted from curvature analysis	2.7±0.43%
Mean phase difference, measured *vs* curvature	31.0±3.7°

Phase difference between strain calculated from midline curvature and strain measured by sonomicrometry is given in degrees per cycle.
Values are means ± s.e.m. for the four fish that met data quality criteria. These fish averaged 42.3±1.1 cm fork length (*L*), and swam at 1.85±0.4 *L* s^{-1} with a tail beat frequency of 2.8±0.12 Hz.

decreased substantially with increasing frequency thereafter, approaching zero after 10 Hz (Fig. 10A). For strain amplitude of ±5.5% contractile power (=work×frequency) had its peak at about 4 Hz, and fell to near zero by 12 Hz (Fig. 10B). Power at 8 Hz and 1 Hz were about equal, but only 30% of the maximum. Very similar results were obtained from muscle sampled at 0.65 *L* (data not shown). Across the frequency range that corresponds to observed tail beat frequencies for steady swimming (~1.8 to 4.0 Hz), power is >70% of maximum (Fig. 10B).

In tests done from 2–6 Hz, net work increased with strain amplitude, approximately doubling when strain was doubled from ±2.75% to ±5.5% (Fig. 9, Fig. 10A). Note that the lower strain used corresponds to that predicted from midline curvature, while the higher strain corresponds to that measured by sonomicrometry. With a further increase in strain to ±8% (a 45% increase over ±5.5% strain) net work was only about 15% higher (data at 3 Hz only; Fig. 9, Fig. 10A). Fig. 11 shows that power output at 3 Hz increased significantly with strain above ±2.75% (*t*-test; $P<0.01$), but power at ±8% was not significantly higher than at ±5.5% (*t*-test; $P>0.05$).

Optimized stimulus phase and duration

The optimal stimulus duration for red muscle in work-loop experiments (i.e. that resulting in maximal net work) averaged 0.3–0.35 of a cycle period between 2 Hz (maximum work) and 4 Hz (maximum power) (Fig. 12A). The optimal activation onset (i.e. phase) required to maximize performance was always during the latter stage of muscle lengthening, ranging from 65–25° at 2 and 4 Hz, respectively (Fig. 12B). These results are comparable to the activation phase and duration recorded in fish swimming in the water tunnel with an average tail beat frequency of 3.2 Hz (Table 2), suggesting that, like skipjack, yellowfin red muscles are not only capable of producing large amounts of work and power *in vitro*, but they are actually used in the manner that appears ideal for doing so *in vivo*. The *in vivo* stimulus duty cycle and phase data were not available until after the work-loop experiments on isolated muscle were complete, so we were unable to test this directly. With increasing cycle frequency the optimal stimulus duty cycle showed a rapid decline, while optimal stimulation phase became more advanced (i.e. closer to zero; see Fig. 12). Both of these effects are an expected consequence of the fact that at higher

Table 2. Activation phase (in degrees) and duration (proportion of cycle period *T*) of deep red muscle relative to the cycle of local strain, determined by comparing EMG burst activity to sonometric traces

Axial position (*L*)	Strain amplitude (±%)	EMG on degrees	EMG off degrees	Duty cycle (*T*)
0.53±0.01	4.9±0.5	50.6±4.5	162.6±5.6	0.31±0.02

Values are reported as means ± standard errors for the five fish that met data quality criteria. These fish averaged 45.0±6.6 cm fork length (*L*), and swam at 1.9±0.3 *L* s^{-1} with a tail beat frequency of 3.2±0.4 Hz.

contraction frequencies the muscle fibres must be activated relatively earlier in the shortening cycle and for a shorter period in order to allow time for force development and relaxation to be completed.

Twitch properties of red and white muscle

The time from stimulus onset to peak force development of isometric twitches was measured to assess potential differences in contractile properties of the red muscles at different axial locations and for comparison with other thunniform swimmers. While our limited success with white muscle preparations does not allow a comprehensive description of the contractile properties of fast fibres, because no twitch or work data from any tuna white muscle have yet been published, we present our results here for preliminary comparison with the performance of red fibres. As expected, white fibres were substantially faster, by about three times, than red fibres (Fig. 13). Red fibres from 0.5 *L* had slightly shorter twitch times than fibres from 0.65 *L* (*t*-test; P=0.03), but this difference was not evident in work or power production spectra.

Preliminary results of work-loop experiments on white fibres (N=2) under stimulus conditions resulting in maximal net work indicated that white muscle is designed to generate power at higher frequencies than is red, with peak power production occurring at 7–8 Hz and positive net power possible up to at least 14 Hz (data not shown).

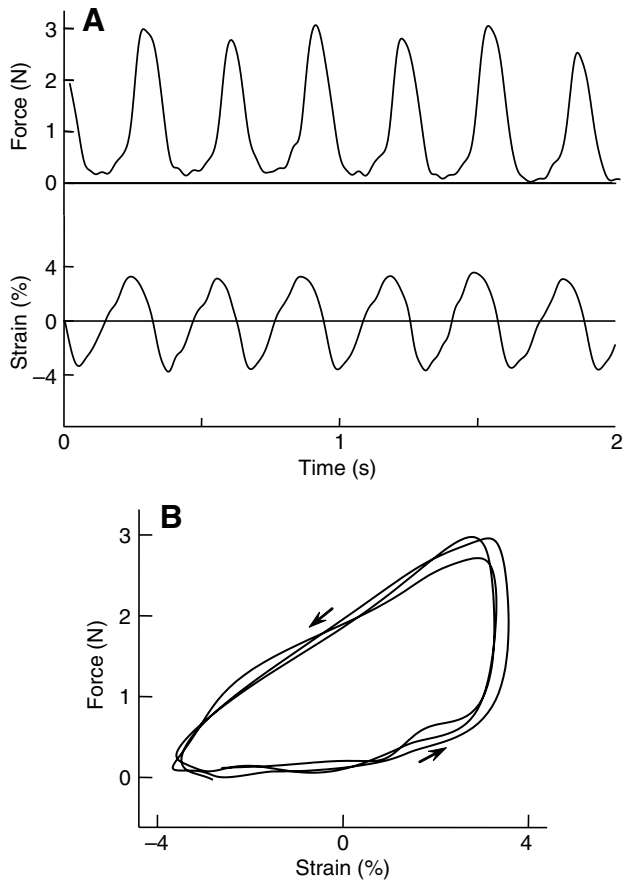

Fig. 7. (A) Example of force measured in the caudal tendons and red muscle length change (expressed as strain) measured at 0.5 *L* in a 45 cm yellowfin tuna swimming at 2.2 *L* s^{-1}. (B) *In vivo* work loop resulting from plot of tendon force and muscle length for three cycles of traces in A.

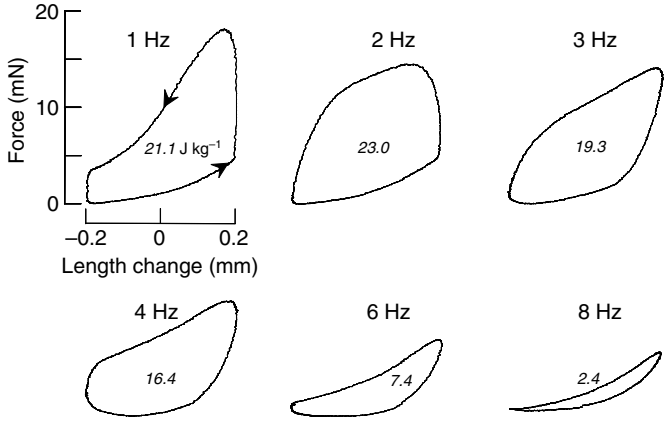

Fig. 8. Examples of work loops obtained from yellowfin tuna red muscle fibers sampled from 0.5 *L*. Rest length was 4.0 mm, strain amplitude for each was ±5.5%; stimulus phase and duration were adjusted to produce maximum net work at each frequency. Values of net work, in J kg^{-1}, are shown in italic type for each frequency. All work loops progress in an anti-clockwise direction (arrows), signifying net positive work. Experiments were conducted at 25°C.

DISCUSSION

Implications for thunniform swimming

This study provides insights into muscle function in yellowfin tuna by use of *in vivo* and *in vitro* techniques, and allows us to make comparisons with muscle performance in faster-swimming skipjack tuna. Previous studies of skipjack employing sonomicrometry revealed a discrepancy between the phase of measured red muscle strain and that calculated from body midline curvature (Shadwick et al., 1999), such that red muscle shortening in the mid body was coincident with curvature and lateral motion of sites about 0.2 *L* more posterior. We note a similar phase shift in the red muscle of yellowfin tuna (Fig. 5 and Table 1). We suggested this posterior phase shift in muscle action was facilitated by highly elongated myomeres and long tendinous connections, not so extreme in other fishes, that allowed

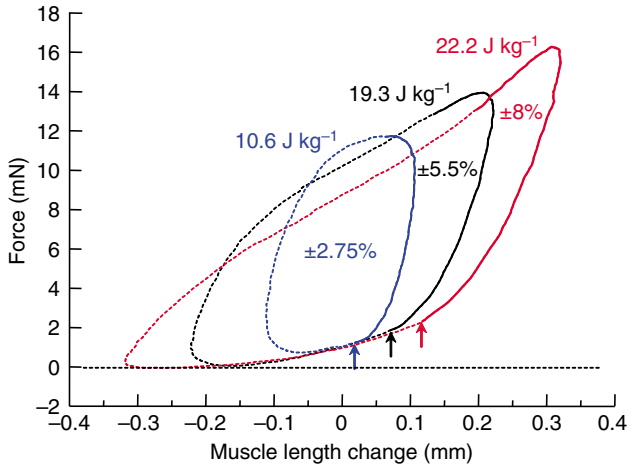

Fig. 9. The effect of strain amplitude on work loops from red muscle taken from 0.5 *L*. Cycle frequency was 3 Hz, strains used were ±2.75, ±5.5, ±8%, and temperature was 25°C. Net work for each strain is shown in J kg^{-1}. Solid line portions of each cycle represent the period when stimulus was on, broken portions are the period when stimulus was off, and arrows indicate stimulus onset.

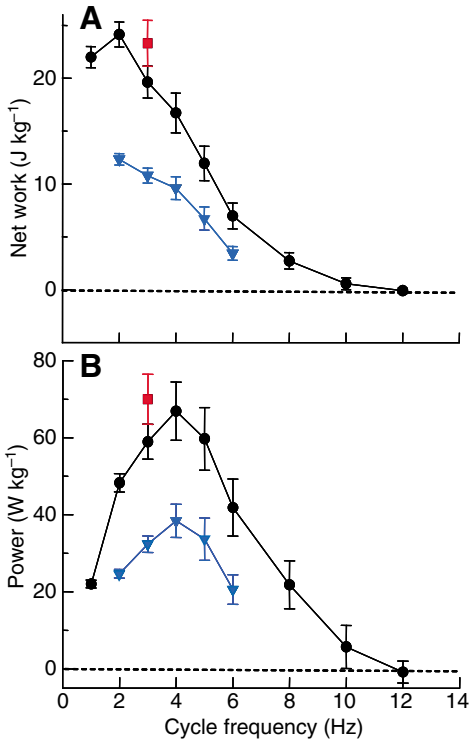

Fig. 10. (A) Net work per cycle *vs* cycle frequency from work loops of yellowfin tuna red muscle optimized for maximum work at 25°C. (B) Net power calculated from data in A. Strains are ±5.5% (black circles), ±2.75% (blue triangles), ±8% (red squares). Values are means ± s.e.m. (*N*=5).

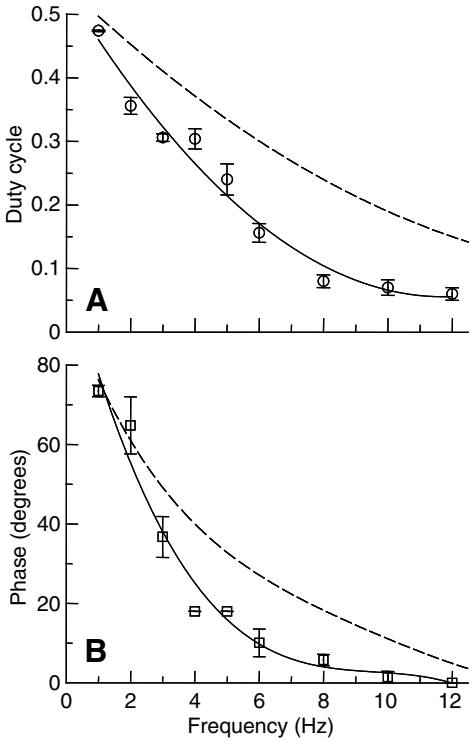

Fig. 12. (A) Stimulus duty cycle and (B) stimulus phase used to obtain maximal work from yellowfin tuna red muscle taken from 0.5 *L* when strain amplitude was ±5.5%. Values are means ± s.e.m. (*N*=5). For comparison, data from skipjack red muscle (Syme and Shadwick, 2002) are included (broken lines). In both cases temperature was held at 25°C.

the red muscle mass to adopt a more anterior and medial position in the body while powering swimming primarily by lateral motions of the caudal fin. This anatomical novelty provides a mechanism for uncoupling the red muscle contractions from local bending so that the lateral motions can be restricted to the caudal region, the essence of 'thunniform' swimming. Recent work on the architecture of the myoseptal tendon system in tunas and other species supports this notion (Gemballa and Konstantinidis, 2005; Shadwick and Gemballa, 2006). Interestingly, lamnid sharks show a remarkable convergence with tunas in their morphology and thunniform swimming mode, as documented by kinematic and anatomical studies (Donley et al., 2004; Donley et al., 2005). It is now clear from structural analysis (S. Gemballa, personal communication) that the positioning of red fibres within the medial tips of the highly elongated myomeres in lamnids

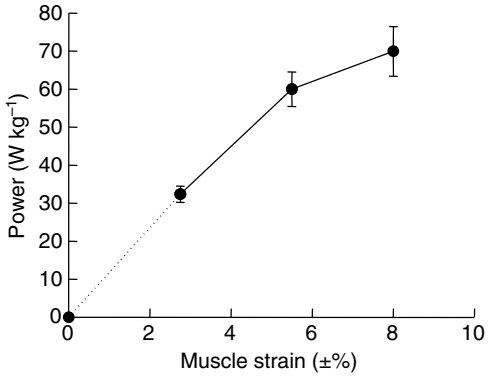

Fig. 11. Net power *vs* strain amplitude for yellowfin tuna red muscle, determined from work loops performed at 3 Hz. Values are means ± s.e.m. (*N*=5). Pairwise comparisons show that power output at ±5.5% and ±8% are not significantly different (*P*>0.05) but both are significantly higher than power at ±2.75% strain (*P*<0.01).

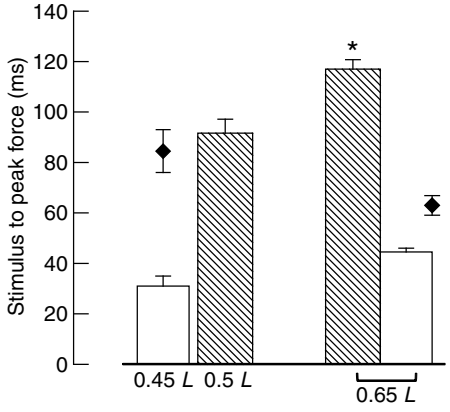

Fig. 13. A comparison of isometric twitch properties of yellowfin tuna red muscle (shaded bars, *N*=5) at 0.5 *L* and 0.65 *L*, and white muscle (white bars, *N*=2) at 0.45 *L* and 0.65 *L*, at 25°C; values are means ± s.e.m. Time to peak force for red muscle was significantly longer at 0.65 *L* (asterisk: *t*-test, *P*=0.03). Twitch times for skipjack red muscle at 0.44 *L* and 0.70 *L* (diamonds) are shown for comparison (Syme and Shadwick, 2002).

and in tunas results in their location appearing to be much more anterior than the rest of the myomere and tendons with which they are associated (Shadwick and Gemballa, 2006; Shadwick, 2005), thus providing the basis for the apparent uncoupling of muscle shortening from local curvature.

As noted in skipjack tuna, the uncoupling of red muscle shortening from local bending (Fig. 5) allows the waves of muscle strain in yellowfin to travel posteriorly along the body at a high velocity relative to swim speed (Shadwick et al., 1999) (Figs 3, 4); consequently muscle shortening is nearly simultaneous along one side of the fish. For example, at a swim speed of 2 $L\ s^{-1}$ the tail beat frequency is about 3 Hz (Fig. 2); the strain wave velocity is about 5.2 $L\ s^{-1}$ (Fig. 4) or 1.7 $L\ T^{-1}$, where T is the tail beat period. Thus, it takes only about 66 ms for the muscle strain wave to propagate along the entire loin of red muscle (i.e. from about 0.35 to 0.7 L). This is slightly slower than what we observed for skipjack (2.5 $L\ T^{-1}$), but similar to strain wave velocities measured in mako sharks [1.4–1.8 $L\ T^{-1}$ (Donley et al., 2005)]. This feature, combined with the elongated myotendinous system, facilitates the characteristic thunniform locomotion, with midbody muscle contractions producing posterior lateral motions. In contrast, muscle strain is coupled to local bending in non-thunniform swimmers so the strain wave velocity is no greater than the propagated wave of bending; for example approximately 0.7 $L\ T^{-1}$ in a trout (Wardle et al., 1995) and 0.85 $L\ T^{-1}$ in a leopard shark (Donley and Shadwick, 2003).

The effect of the special situation in the tuna is demonstrated by *in vivo* muscle 'work loops' (Fig. 7). Tunas are the only fish with large discrete tendons that have been instrumented for direct muscle force measurements during swimming (Knower et al., 1993; Shadwick et al., 2002a). The close synchrony between muscle shortening in the mid-body and force development in the caudal tendons is evident; the resulting work loop is large and positive net work is produced, like the optimized work loops of isolated muscle fibres (Figs 8, 9).

The functional uncoupling of tuna red muscle contractions from local curvature results in an additional novelty; shortening strains are greater than predicted from body curvature in yellowfin (Fig. 5 and Table 1) (Katz et al., 2001) and in skipjack (Shadwick et al., 1999). In the current study deep red muscle strain at 0.5 L was twice that predicted based on body curvature. In fact, strain in the deep location was even greater than the strain predicted from curvature if the fibres occupied a superficial position, as in other fish (Shadwick et al., 2002b; Katz, 2002). Thus, the internalization of the red fibres does not reduce active shortening work per cycle, or power output, as would be expected under the anatomical regime found in other fish. To quantify this prediction we compared work and power production from isolated red fibres in work-loop experiments at strains representing the average measured *in vivo* using sonomicrometry (±5.5%) and that predicted based on local body curvature assuming muscle strain as in a homogenous material (±2.7%). The results show the benefit of the unique muscle anatomy in the tuna; work and power output are twice as high as they would be if the red muscle occupied its medial position, but did not have the connective tissue framework that allows its contractions to be directed to the caudal region (Figs 9–11) rather than cause local bending. Further increases in strain amplitude above that measured *in vivo* result in only a modest increase in work and power output (Figs 9–11). These observations are particularly intriguing in the context of the evolution of this body form, particularly the acquisition of regional endothermy. It has been hypothesized that the shift in red muscle position from superficial to medial and anterior preceded the development of the vascular counter-current heat exchanger that now elevates core body temperature in tunas and lamnid sharks (Graham and Dickson, 2000; Bernal et al., 2001). Our results suggest that a specific biomechanical advantage was realized by the anterior and medial shift of the red fibres, supporting the notion that selection for improved swimming performance could have occurred independent of any advantage conferred by regional endothermy.

Performance of red muscle *in vitro*

Our estimate of maximum power produced by red muscle of yellowfin tuna from work loops at a strain of ±5.5% is approximately 66 W kg^{-1} at 0.5 L and 63 W kg^{-1} at 0.65 L. This is comparable to results from a similar study on skipjack red muscle in which maximum power output ranged from 44 to 75 W kg^{-1} between axial positions of 0.44 and 0.7 L (Syme and Shadwick, 2002). However, these values are substantially higher than those reported (Altringham and Block, 1997) in a work loop study of yellowfin red muscle (12 W kg^{-1} at ±5% strain and 25°C). While there are undoubtedly some differences arising from experimental procedure, we believe the most likely explanation for this discrepancy is in the determination of muscle mass. Altringham and Block measured wet muscle mass directly (Altringham and Block, 1997) and, if there are substantial amounts of non-viable tissue in the preparations, then active muscle mass would have been overestimated. With our technique of estimating functional cross-sectional area (and mass) from isometric stress this potential problem is avoided [for a detailed discussion, see Syme and Shadwick (Syme and Shadwick, 2002)]; however assumptions about area-specific force may not apply universally across different species and muscles, reducing the rigor of such comparisons.

Muscle function in yellowfin *vs* skipjack tunas

The current study demonstrates differences in muscle mechanics of yellowfin and skipjack tuna that support previous observations on differences in their swimming behaviour, specifically their aerobic speed range. Firstly, the minimum speed needed to maintain hydrodynamic equilibrium is based on the lift generated by pectoral fins, which are significantly larger in yellowfin than in skipjack; thus yellowfin minimum cruising speed is lower (Magnuson, 1978). In captivity the undisturbed routine cruising speed is also typically lower in yellowfin, at about 1 $L\ s^{-1}$ (this study) (Altringham and Block, 1997) *vs* 1.8 $L\ s^{-1}$ for skipjack (Gooding et al., 1981; Syme and Shadwick, 2002). In laboratory tests of 40–50 cm fish, yellowfin have a lower

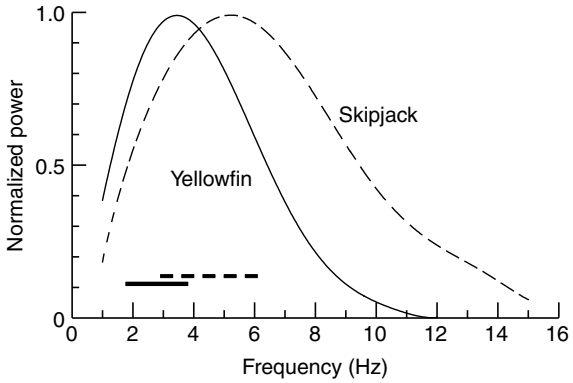

Fig. 14. Comparison of power curves for red muscle from yellowfin (solid line) and skipjack (broken line), normalized by maximum power for each. Both at 25°C. Horizontal bars represent the range of tail beat frequencies observed during unrestrained cruise swimming in yellowfin (solid line) and skipjack (broken line). Data for skipjack are from previous work (Syme and Shadwick, 2002).

maximum aerobic swim speed, at about 2.5 $L\ s^{-1}$, than do skipjack at about 3.7 $L\ s^{-1}$ (Dewar and Graham, 1994; Knower et al., 1999). These speed ranges correspond to a range of tail beat frequencies and their associated cycle frequencies in the work-loop experiments. A comparison of the range of aerobic cycle (tail beat) frequencies for the two species and the respective muscle power output at these frequencies (Fig. 14) demonstrates that power output is maximized at higher frequencies in skipjack than in yellowfin and that both species employ tail beat frequencies during cruise swimming that result in near-maximal or maximal power output from the red muscle.

Our findings also suggest that specific differences in muscle contractile properties contribute to the observed differences in sustained swimming speeds. For example, support for this premise is seen by comparing the optimized timing of activation for work output between the species (Fig. 12); yellowfin muscle must be activated earlier in the strain cycle and for a shorter duration than skipjack muscle, a characteristic of slower force development (Fig. 13) and most likely slower relaxation times. Interestingly, the average phase delay between muscle strain and midline curvature during swimming was less in the yellowfin (31°; Table 1) than it was in skipjack [48° (Shadwick et al., 1999)], possibly reflecting more elongate myomeres and/or connective tissue linkages in the latter which may also enhance the capacity for faster swimming.

Manoeuvrability

While the specializations described above equip tunas to swim fast, they also reduce manoeuvrability. The bulky cross section and relatively stiff vertebral column of tunas compromise turning and sudden accelerations (Blake, 2004). Furthermore, the medial red muscles in tunas are designed to transmit power to the tail by the elongated tendons, making them less effective in steering because they do not cause local bending. As noted in earlier studies, sudden accelerations and turns are powered solely by the caudal fin (Fierstine and Walters, 1968), so turning while cruising requires a large radius, nearly 0.5 L (Blake et al., 1995), or 2–3 times greater than for carangiform or sub-carangiform species (Webb and Keyes, 1981). Consequently, tuna red muscles are primarily used for forward propulsion, apparently permitting them to operate at or near maximal power, unlike other fishes in which red myotomal muscles also aid in steering, which may preclude them from operating near maximal power. Indeed, all the evidence points to non-thunniform swimmers producing far less than maximal power with their red muscles (Syme et al., 2008) (reviewed by Altringham and Ellerby, 1999; Coughlin, 2002; Syme, 2006). Thus, tunas appear to have opted for speed over manoeuvrability, a strategy well suited to their niche as open water predators.

The authors wish thank Richard Brill for his tireless efforts to help visiting scientists at the Kewalo Research Facility where this work was carried out, Jeff Graham for the use of the water tunnel, Steve Katz for helpful discussions and assistance with aspects of the *in vivo* research program, Andy Biewener for the tendon buckles, and Brad Shadwick for developing the curvature analysis software. We are grateful for financial support from NSF (IBN 95-14203 and IBN 00-91987 to R.S.) and NSERC (to D.S. and R.S.).

REFERENCES

Altringham, J. D. and Block, B. A. (1997). Why do tuna maintain elevated slow muscle temperatures? Power output of muscle isolated from endothermic and ectothermic fish. *J. Exp. Biol.* **200**, 2617-2627.

Altringham, J. D. and Ellerby, D. J. (1999). Fish swimming: patterns in muscle function. *J. Exp. Biol.* **202**, 3397-3403.

Altringham, J. D. and Shadwick, R. E. (2001). Swimming and muscle function. In *Fish Physiology, Vol.* 19, *Tuna: Physiology, Ecology and Evolution* (ed. B. A. Block and E. D. Stevens), pp. 313-344. San Diego: Academic Press.

Altringham, J. D. and Young, I. S. (1991). Power output and the frequency of oscillatory work in mammalian diaphragm muscle: the effects of animal size. *J. Exp. Biol.* **157**, 381-389.

Bernal, D., Dickson, K. A., Shadwick, R. E. and Graham, J. B. (2001). Analysis of the evolutionary convergence for high performance swimming in lamnid sharks and tunas. *Comp. Biochem. Physiol.* **129A**, 695-726.

Blake, R. W. (2004). Fish functional design and swimming performance. *J. Fish Biol.* **65**, 1193-1222.

Blake, R. W., Chatters, L. M. and Domenici, P. D. (1995). Turning radius of yellowfin tuna (*Thunnus albacares*) in unsteady swimming manoeuvres. *J. Fish Biol.* **46**, 536-538.

Coughlin, D. J. (2000). Power production during steady swimming in largemouth bass and rainbow trout. *J. Exp. Biol.* **203**, 617-629.

Coughlin, D. J. (2002). Aerobic muscle function during steady swimming in fish. *Fish Fish.* **3**, 63-78.

Dewar, H. and Graham, J. B. (1994). Studies of tropical tuna swimming performance in a large water tunnel. I. Energetics. *J. Exp. Biol.* **192**, 13-31.

Donley, J. M. and Shadwick, R. E. (2003). Steady swimming muscle dynamics in the leopard shark *Triakis semifasciata*. *J. Exp. Biol.* **206**, 1117-1126.

Donley, J. M., Sepulveda, C. A., Konstantinidis, P., Gemballa, S. and Shadwick, R. E. (2004). Convergent evolution in mechanical design of lamnid sharks and tunas. *Nature* **429**, 61-65.

Donley, J. M., Shadwick, R. E., Sepulveda, C. A., Konstantinidis, P. and Gemballa, S. (2005). Patterns of red muscle strain/activation and body kinematics during steady swimming in a lamnid shark, the shortfin mako (*Isurus oxyrinchus*). *J. Exp. Biol.* **208**, 2377-2387.

Ellerby, D. J., Spierts, I. L. Y. and Altringham, J. D. (2001). Fast muscle function in the European eel (*Anguilla anguilla* L.) during aquatic and terrestrial locomotion. *J. Exp. Biol.* **204**, 2231-2238.

Fierstine, H. L. and Walters, V. (1968). Studies in locomotion and anatomy of scombroid fishes. *Mem. South Calif. Acad. Sci.* **6**, 1-31.

Gemballa, S. and Konstantinidis, P. (2005). Derived trunk morphology in a thunniform swimmer: the musculotendinous system of *Euthynnus alletteratus*. *Comp. Biochem. Physiol.* **141A**, S170-S171.

Gooding, R. M., Neill, W. H. and Dizon, A. E. (1981). Respiration rates and low oxygen tolerance limits in skipjack tuna, *Katsuwonus pelamis*. *U. S. Fish. Bull.* **79**, 31-48.

Graham, J. B. and Dickson, K. A. (2000). The evolution of thunniform locomotion and heat conservation in scombrid fishes: new insights based on the morphology of *Allothunnus fallai*. *Zool. J. Linn. Soc.* **129**, 419-466.

Graham, J. B. and Dickson, K. A. (2004). Tuna comparative physiology. *J. Exp. Biol.* **207**, 4015-4024.

James, R. S., Altringham, J. D. and Goldspink, D. F. (1995). The mechanical properties of fast and slow skeletal muscles of the mouse in relation to their locomotory function *J. Exp. Biol.* **198**, 491-502.

Josephson, R. K. (1985). Mechanical power output from striated muscle during cyclic contraction. *J. Exp. Biol.* **114**, 493-512.

Katz, S. L. (2002). Design of heterothermic muscle in fish. *J. Exp. Biol.* **205**, 2251-2266.

Katz, S. L. and Shadwick, R. E. (1998). Curvature of swimming fish midlines as an index of muscle strain suggests swimming muscle produces net positive work. *J. Theor. Biol.* **193**, 243-256.

Katz, S. L., Shadwick, R. E. and Rapoport, H. S. (1999). Muscle strain histories in swimming milkfish in steady as well as sprinting gaits. *J. Exp. Biol.* **202**, 529-541.

Katz, S. L., Syme, D. A. and Shadwick, R. E. (2001). High speed swimming: enhanced power in yellowfin tuna. *Nature* **410**, 770-771.

Knower, T., Shadwick, R. E., Biewener, A. A., Korsmeyer, K. and Graham, J. B. (1993). Direct measurement of tail tendon forces in swimming tuna. *Am. Zool.* **3**, 30A.

Knower, T., Shadwick, R. E., Katz, S. L., Graham, J. B. and Wardle, C. S. (1999). Red muscle activation patterns in yellowfin (*Thunnus albacares*) and skipjack (*Katsuwonus pelamis*) tunas during steady swimming. *J. Exp. Biol.* **202**, 2127-2138.

Magnuson, J. J. (1978). Locomotion by scombroid fishes. Hydromechanics, morphology and behavior. In *Fish Physiology*. Vol. VII (ed. W. S. Hoar and D. J. Randall), pp. 239-313. New York: Academic Press.

Shadwick, R. E. (2005). How tunas and lamnid sharks swim: an evolutionary convergence. *Am. Sci.* **93**, 524-531.

Shadwick, R. E. and Gemballa, S. (2006). Muscle dynamics in fish. In *Fish Physiology*, *Vol. 23, Fish Biomechanics* (ed. R. E. Shadwick and G. V. Lauder), pp. 241-280. San Diego: Academic Press.

Shadwick, R. E., Katz, S. L., Korsmeyer, K. E., Knower, T. and Covell, J. W. (1999). Muscle dynamics in skipjack tuna: timing of red muscle shortening in relation to activation and body curvature during steady swimming. *J. Exp. Biol.* **202**, 2139-2150.

Shadwick, R. E., Rapoport, H. S. and Fenger, J. M. (2002a). Structure and function of tuna tail tendons. *Comp. Biochem. Physiol.* **133A**, 1109-1125.

Shadwick, R. E., Syme, D. A. and Katz. S. L. (2002b). Thunniform swimming: muscle dynamics and mechanical power production by aerobic fibers of yellowfin tuna (*Thunnus albacares*). *Physiologist* **45**, 310.

Syme, D. A. (2006). Functional properties of skeletal muscle. In *Fish Physiology*, *Vol.* 23, *Fish Biomechanics* (ed. R. E. Shadwick and G. V. Lauder), pp. 79-240. San Diego: Academic Press.

Syme, D. A. and Shadwick, R. E. (2002). Effects of longitudinal body position and swimming speed on mechanical power of deep red muscle from skipjack tuna (*Katsuwonus pelamis*). *J. Exp. Biol.* **205**, 189-200.

Syme, D. A., Gollock, M., Freeman, M. J. and Gamperl, A. K. (2008). Power isn't everything: muscle function and energetic costs during steady swimming in Atlantic cod (*Gadus morhua*). *Physiol. Biochem. Zool.* **81**, doi: 10.1086/528784.

van Leeuwen, J. L., Lankheet, M. J. M., Akster, H. A. and Osse, J. W. M. (1990). Function of red axial muscles of carp (*Cyprinus carpio*): recruitment and normalized power output during swimming in different modes. *J. Zool.* **220**, 123-145.

Wardle, C. S., Videler, J. J. and Altringham, J. D. (1995). Tuning in to fish swimming waves: body form, swimming mode and muscle function. *J. Exp. Biol.* **198**, 1629-1636.

Webb, P. W. and Keyes, R. S. (1981). Division of labour between median fins in swimming dolphin (Pisces: Coryphaeidae). *Copeia* **4**, 901-904.